

Photo-Activated Luminescence of CdSe Quantum Dot Monolayers

S. R. Cordero, P. J. Carson, R. A. Estabrook, G. F. Strouse, and S. K. Buratto*

Department of Chemistry and Biochemistry, University of California, Santa Barbara, California 93106-9510

Received: May 11, 2000; In Final Form: August 8, 2000

We show that the luminescence from CdSe quantum dot monolayers can be strongly influenced by the interaction of water molecules adsorbed on the surface. Light-induced alterations in the surface states following adsorption of water, results in quasi-reversible luminescence changes in the quantum dot. The excitonic QY increases by a factor of 20 during the first 200 s of illumination in air (post vacuum) and then steadily decreases to a level 6 times that of the vacuum reference after 5000 s. The exciton emission exhibits an exponential blue shift of nearly 16 nm (60 meV) over 1 h of illumination. During this time, the line width decreases by 10% during the first 100 s and then slowly increases to 96% of the vacuum reference line width after 5000 s. Our model suggests that water molecules adsorbed on the surface of the quantum dot act to passivate surface traps, which results in increased luminescence, similar to an effect well-known for bulk CdSe surfaces. In addition, adsorbed water molecules act to oxidize the surface of the quantum dot, which results in the blue shift of the exciton emission and eventually introduces new surface defects that lower the luminescence. It is the competition between these two processes that is responsible for the complex kinetics of the luminescence QY.

I. Introduction

Nanocrystals of II–VI semiconductors (CdS, CdSe, CdTe) prepared as colloids in the 1–10 nm size range have generated tremendous interest over the past decade in the fields of physics, chemistry, and engineering.^{1–8} These nanocrystals are prototypical quantum dots with their electronic structure dependent on quantum confinement effects in all three spatial dimensions.⁹ As a result, the optical properties are dramatically different than the bulk material. In addition, these quantum dots are of technological interest as the active material in optical or optoelectronic devices such as optical switches, light-emitting diodes (LEDs), and lasers.^{1,9,10} Over the past seven years, the synthetic methods have progressed such that high quality samples can be prepared in large quantities with narrow size distributions, controlled surface chemistry, and functionality.^{11,12} Current interest in this field is directed toward the preparation of ordered arrays of quantum dots in two or three dimensions^{4,10,13–15} in order to probe cooperative effects between quantum dots such as inter-dot coupling, energy transfer, electron transfer, and collective excitation.^{10,16,17}

At the center of interest in II–VI quantum dots is their luminescence properties, which are sensitive to surface interactions in these materials. While high luminescence quantum yields (approaching 50%) have been quoted for core/shell CdSe/CdS quantum dots, typical quantum yields (QY) are in the 1–10% range.^{12,18} Furthermore, the dependence of the emission on the quantum dot surface is not completely understood, but the degree of surface passivation has been shown to be a crucial parameter in determining the luminescence QY.¹⁹ In addition, surface passivation is even more critical in quantum dot solids where inter-dot coupling reduces the QY of the film by over a factor of 10 relative to that of the colloid.¹⁵ In this paper, we show that the luminescence properties of ordered monolayers of 4.1 nm CdSe quantum dots capped with hexadecylamine (HDA) can be enhanced by over an order-of-magnitude by surface adsorbates, specifically water. We have found similar

results in TOP/TOPO and ZnS (core/shell) materials. This effect is quasi-reversible and is similar to the enhancement in the luminescence observed for both hexametaphosphate stabilized CdS nanoclusters sandwiched between monolayers of dioctadecyldimethylammonia bromide²⁰ and that of bulk CdSe surfaces covered with electron-donating molecules (Lewis bases).^{21,22}

II. Sample Preparation and Characterization

The CdSe quantum dots were prepared using a slight variation on the lyothermal synthesis developed by Bawendi and co-workers.^{12,23} Size-selective precipitation and removal of excess HDA results in a distribution of HDA-capped CdSe nanocrystals with a mean size of 4.1 nm and an root-mean-square (rms) width of 7–8% (± 0.16 nm). Strict inert conditions were followed during all preparations steps. The CdSe nanocrystals are deposited from hexane at the air–water interface using a Langmuir film balance. Compression of the film results in a pressure–area isotherm as shown in Figure 1a. The film is transferred to a clean glass cover slip by the Schaeffer lift-off method¹⁰ at a surface pressure of 30 mN/m. Transmission electron microscopy (Figure 1(b)) shows that the films are close-packed glasses with ordered domains of quantum dots on the 100 nm scale. The absorption spectrum of both the colloidal suspension in hexane and the monolayer are similar as seen from Figure 1(c).

Luminescence spectra are acquired from the quantum dot monolayers in a modified fluorescence microscope. Here, the samples are placed inside a small vacuum chamber, which has a glass view port and a back-fill inlet. The illumination source is light from a Xe arc lamp (75 W) filtered for 400–490 nm excitation, and then passed through a 10x/0.4 numerical aperture (NA) microscope objective (power ≈ 3 W/cm²). Using the microscope in reflection geometry, the luminescence is collected with the objective and routed to a CCD-spectrometer via a multi-mode optical fiber. Using this configuration, spectra are captured repetitively with various integration times. Luminescence spectra

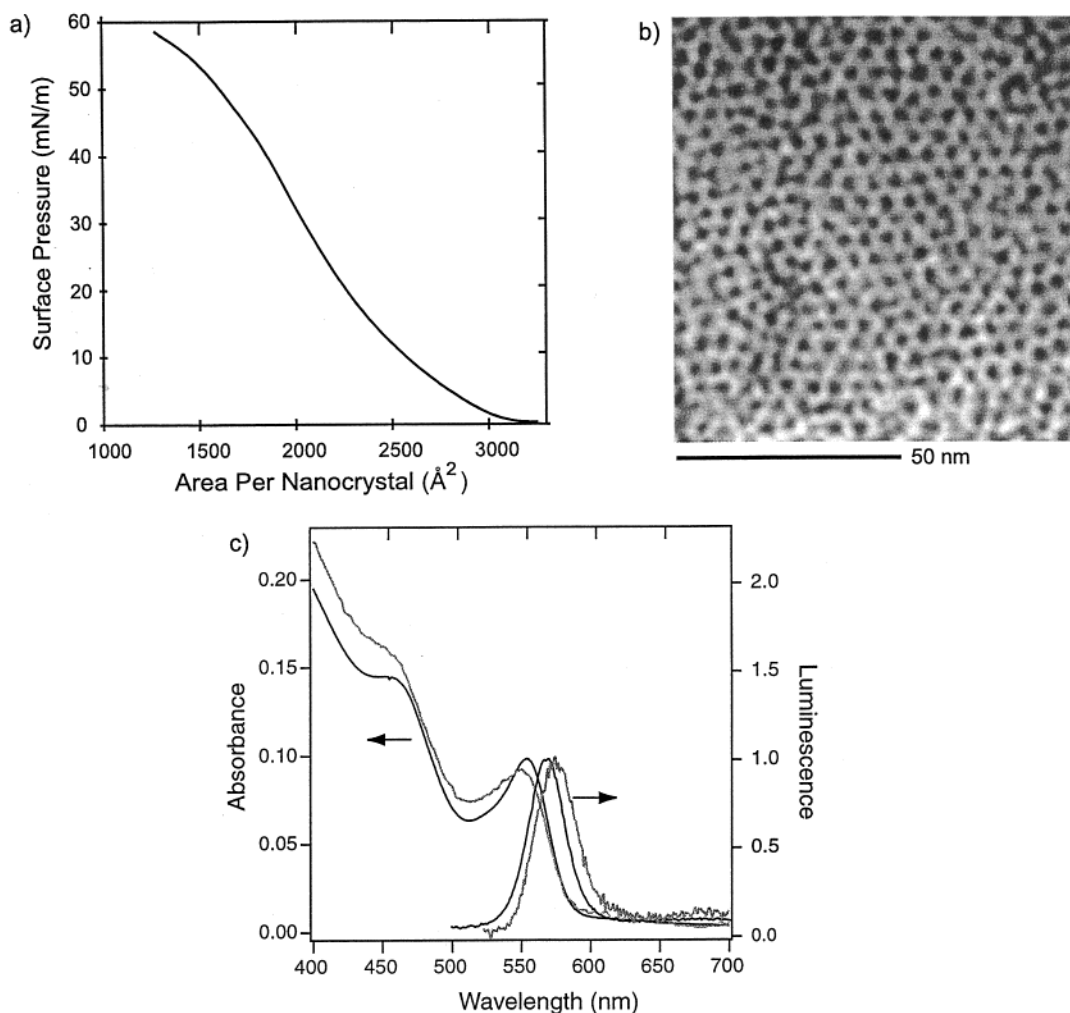


Figure 1. Typical surface pressure–area isotherm of 4.1 nm HDA-capped CdSe quantum dots taken at room temperature (part a). Transmission electron micrograph of monolayer film showing hexagonal close-packing on a ~ 100 nm length scale (part b). Absorbance and the normalized luminescence spectra (part c) of the quantum dot colloidal solution (shown in black) and the monolayer film (shown in gray). The absorbance spectrum of the monolayer is multiplied by a factor of 6 in order for it to be on the same scale as the colloidal solution spectrum.

of the colloidal solution in hexane and the monolayer are shown in Figure 1(c).

III. Results and Discussion

Luminescence spectra from a CdSe quantum dot monolayer at different illumination times in air are shown in Figure 2(a). Initially the monolayer is held at a pressure of 10^{-5} Torr to establish a reference point. The emission spectrum at this vacuum pressure is expanded in the inset of Figure 2(a). Note that under these conditions, two luminescence peaks are observed; the narrow exciton emission centered at 580 nm and the broad deep trap emission centered near 730 nm. The deep trap emission is attributed to emission from mid-gap states that arise from surface defects or un-passivated surface atoms² and will be discussed further later in the text. The QY of the as-transferred and dried quantum dot monolayers has been measured, using an integrating sphere, to be 0.4%.²⁴ This represents an 18-fold decrease in QY relative to the QY of the colloid in de-gassed solvent (7%), which is consistent with other experiments on quantum dots. In addition, the deep trap emission represents more than half of the total emission of the film in a vacuum while it represents less than 1% of the total emission of the colloidal solution.

The time dependence of the exciton emission was extracted from fits to the spectra in the region from 500 to 710 nm. In

the absence of an exact model for the line shapes of the exciton peak and the defect peak, assumptions were made about the extent of their overlap with each other. Each peak was fit to multiple Gaussians, constrained in such a way as to ensure that they did not slide excessively during the fit out of the region of the peak they were assigned to. The total area of the exciton peak is plotted in the curve discussed above in Figure 2(b), representing fits to 990 spectra, 5.2 s each.

Once the chamber is vented to room air, the excitonic luminescence signal rises to a maximum value 20 times that of the vacuum reference during the first 200 s (QY = 8%) and then falls to a nearly asymptotic value 6 times that of the vacuum reference (QY = 2.4%). Given that the solution QY is 7%, the QY of the monolayer reaches a maximum nearly equal to or slightly greater than that of the solution. Note also that the deep trap emission is a much smaller fraction of the total luminescence for the spectra of Figure 2(a)-2 and 2(a)-3, indicating that the increase in the luminescence QY comes primarily from an increase in the exciton emission QY. The rising luminescence in Figure 2(b) is exponential with a time constant of 52 s. The luminescence decay after 200s is double exponential with equally weighted time constants of 560 and 2300 s.

Further analysis of the fits to the luminescence spectra reveals changes in both the average position and rms line width (twice the standard deviation) of the exciton emission (Figure 3). The

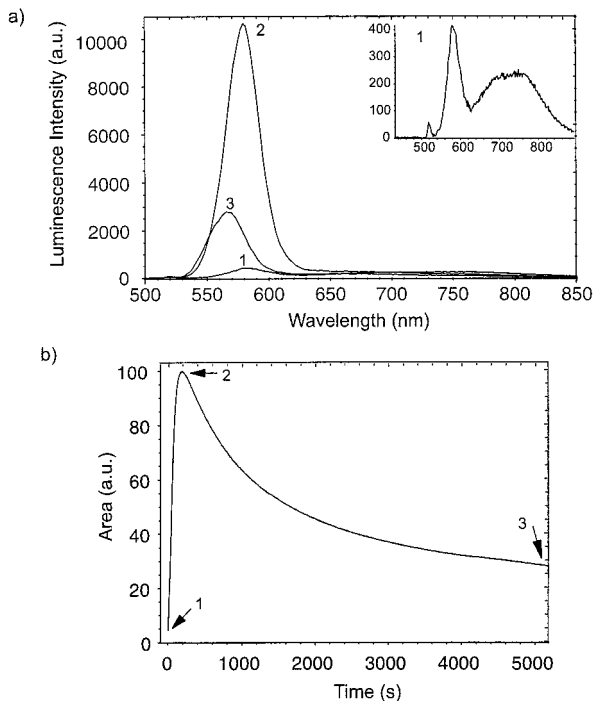


Figure 2. Representative luminescence spectra (part a), and the exciton emission intensity as a function of illumination time in air (part b). Representative spectra were taken at the times labeled by arrows in part b. The luminescence spectrum acquired before venting (arrow 1) is shown in the inset with the y-axis expanded. The small peak at 520 is an artifact of the instrument. Just after time 1 the vacuum chamber (10^{-5} Torr) is vented to the room air (1 atm). The photoluminescence rise is fit to a single exponential with a time constant of 52 s, and the decay is fit to two exponentials with time constants of 560 and 2300 s respectively.

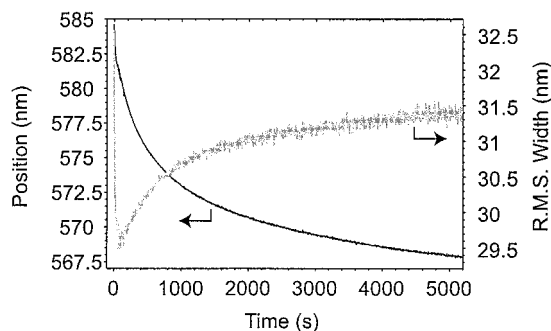


Figure 3. First-moment (average position) of the exciton emission peak (black) and (gray) the rms width both vs illumination time in air. The change in average position fits well to a double exponential with time constants of 450 s and 3100 s. Note that the peak position shifts 16 nm (~ 60 meV) to the blue over the course of the experiment. The rms width exhibits similar (but inverted) kinetics to the luminescence intensity of Figure 2(a) and is fit to a single-exponential decay with time constant 31 s and a double exponential rise with time constants of 560 s and 11 500 s.

average position of the exciton peak shifts to the blue by ~ 16 nm (60 meV) with increasing illumination in air and is still shifting after 5000 s of illumination. After complex dynamics in the first 300 s, this curve fits well to a double exponential decay with time constants of 450 and 3100 s, each with the nearly equal weighting. This blue shift is a strong indication that the size of the quantum dots is getting smaller presumably due to photochemistry. A gradual blue shift of CdSe quantum dots illuminated in air has been previously observed in room-temperature luminescence from single quantum dots and attributed to photooxidation of the surface.⁷

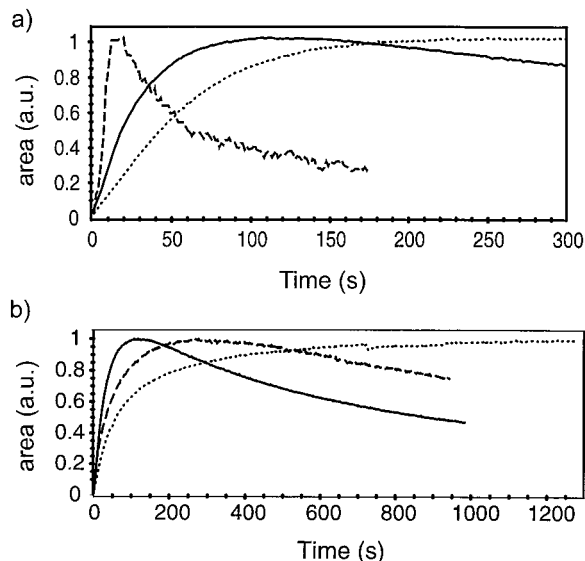


Figure 4. Luminescence from quantum dot monolayers fabricated from different size quantum dots (part a) and for monolayers fabricated from 4.1 nm quantum dots with different capping ligands (part b). Part (a) shows the kinetics of the luminescence quantum yield for monolayers fabricated from 2.8 nm (dashed line), 4.1 nm (solid line) and 6 nm (dotted line) quantum dots. Part (b) shows the kinetics of the luminescence quantum yield for monolayers fabricated from 4.1 nm quantum dots capped with HDA (solid line), capped with TOP/TOPO (dashed line), and 4.1 nm core/shell (CdSe/ZnS) quantum dots capped with TOP/TOPO.

The spectral width undergoes an even more complex evolution. During the first 100 s, the rms line width of the spectrum decreases by $\sim 10\%$ and then increases over the next 5000 s to 96% of the original width. This curve fits well to a single exponential decay with time constant 31 s and a double exponential rise with equally weighted rise constants of 560 and 11500 s. It is important to note that the kinetics of the change in luminescence intensity and the change in spectral width are similar. The luminescence QY and the rms line width show a local maximum and local minimum, respectively. This indicates the possibility of competing mechanisms for the photophysics.

Similar effects on the luminescence have been observed for monolayers fabricated from different size quantum dots and from 4.1 nm quantum dots with different capping ligands (see Figure 4). The dependence on quantum dot diameter is presented in Figure 4a, which shows the integrated intensity as a function of illumination time in air. All of the curves in Figure 4a can be fitted two a biexponential rise and a single exponential decay. The main difference between the three curves is in the exponential decay constant which is largest for the 2 nm quantum dots and smallest for the 6 nm quantum dots. The dependence on the capping ligand is presented in Figure 4b. These data show that the kinetics of the HDA-capped quantum dots and the TOP/TOPO-capped quantum dots are similar. Each shows the familiar biexponential rise and a single exponential decay with only subtle differences in the decay constants between the HDA-capped and the TOP/TOPO-capped quantum dots. If the 4.1 nm CdSe quantum dots are first capped with a few monolayers of ZnS in a core-shell geometry prior to capping with HDA or TOP/TOPO, then the kinetics are changed more dramatically. In this case, only the biexponential rise is observed and not the single-exponential decay over the 30 min of illumination. In addition, no blue-shift of the exciton emission is observed for monolayers of the core-shell quantum dots. This implies that the photooxidation responsible for the eventual

TABLE 1: Various Gases Independently Introduced into the Vacuum Chamber along with the Resulting Photoluminescence Increase (relative to vacuum)

gas	argon					
	dry	CO ₂ dry	N ₂ dry	O ₂ dry	N ₂ (H ₂ O)	O ₂ (H ₂ O)
relative PL	1	1	1	1	8	7.8

^a The gases labeled “dry” were passed through a gas drying unit, while the gases labeled “H₂O” were bubbled through de-ionized water.

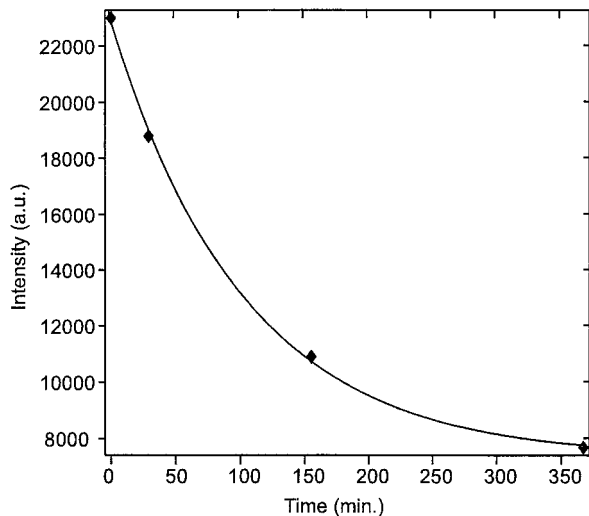


Figure 5. Luminescence intensity versus delay time in the dark. The sample is initially illuminated in order to reach a maximum level and then left in the dark for a time represented on the *x*-axis. The luminescence intensity is monitored at each point with a brief, 1 s integration. The decay fits well to a single exponential with a characteristic decay time of 100 min.

decay of the luminescence QY, and the blue shift of the exciton emission does not occur in the core shell quantum dots, a conclusion consistent with other groups.

We have determined that the activation is strongly dependent on the atmospheric conditions as seen in Table 1. To determine the atmospheric constituent taking part in the activation process, the following experiments were performed. Beginning at a vacuum reference point (10^{-5} Torr), we vented the sample chamber to a variety of atmospheric gases including dry Ar, dry N₂, dry O₂, dry CO₂, wet N₂ (N₂ bubbled through deionized water), and wet O₂ and monitored the evolution of the luminescence. No photoactivation was observed for any of the dry gases, but both wet N₂ and wet O₂ exhibited activation nearly identical to that observed in Figure 2a. Furthermore, the total increase in luminescence efficiency for exposure to wet N₂ and wet O₂ was the same. These results indicate that it is the water present in ambient air, which is taking part in the photoactivation process. It should be possible to quantify the photoactivation effect by adjusting the relative humidity of the venting gases. We are currently preparing such experiments.

Exposure to air without light is not sufficient to activate luminescence even at elevated temperatures. Furthermore, evidence that the luminescence activation is light-induced is seen in Figure 5, which shows the luminescence intensity as a function of delay time in the dark. In this experiment, the CdSe monolayer was activated by illuminating the film in air until a maximum in the luminescence timecourse was reached. The illumination source was then shuttered off, and the film remained in the dark. Emission measurements were periodically performed on the sample. As is clearly observed, the luminescence QY decays exponentially as a function of time in the dark with a characteristic time constant of 6000 s. We have also observed

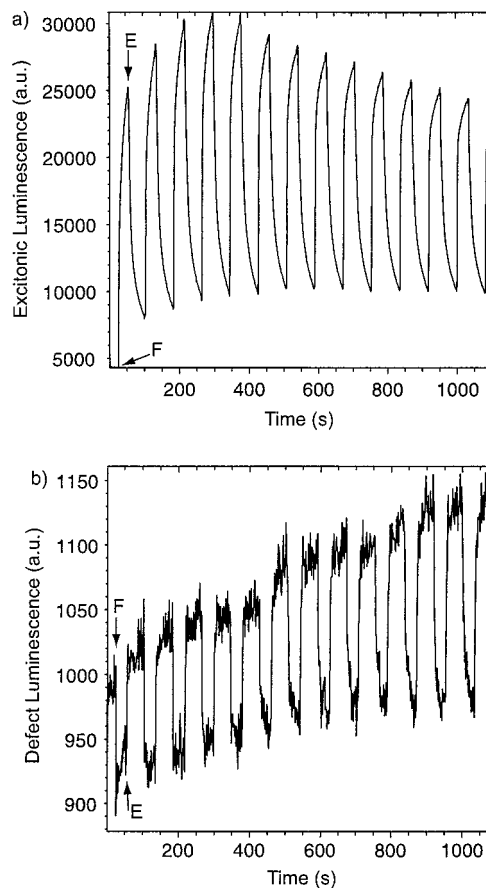


Figure 6. Effect of pressure cycling on the luminescence quantum yield. The exciton emission intensity (part a) and the defect emission intensity (part b) are plotted for 13 cycles of the pressure between 10^{-5} Torr and 1 atm of air. Pressure is cycled by (F) filling for 30 s and (E) evacuating for 50 s. The exciton emission increases for each high-pressure cycle and decreases for each low-pressure cycle. The defect emission, on the other hand, decreases for each high-pressure cycle and increases for each low-pressure cycle. The steady increase in the defect emission over time and the envelope of the exciton emission maxima (which is similar to the plot in Figure 2(a)) is indicative that the activation phenomenon is not completely reversible.

that the film can be reactivated by simply restoring the illumination, which suggests that the activation process is repeatable, and that the de-activation in the dark is not simply irreversible degradation of the quantum dots in air.

To test the reversibility of the activation, we placed a CdSe monolayer in a vacuum, vented the sample chamber to air and monitored the luminescence for approximately 30 s. After 30 s, the vent was closed and the vacuum was restored and held for approximately 50 s. During the time in a vacuum, the luminescence was also monitored. This cycle was then repeated 13 times, and the evolution of the luminescence is shown in Figure 6. It is important to note that venting occurs on the time scale of seconds. However, evacuation was found to take nearly 100 s (to go from 1 atm to 10^{-5} Torr). Figure 6(a) shows the evolution of the exciton emission intensity during exposure to air and to vacuum. During the periods in air, the intensity of the exciton emission increases with kinetics similar to that observed in Figure 2(b). During the periods in vacuum, the exciton emission falls exponentially. The de-activation of the exciton emission occurs on a slower time scale than the activation, compared with Figure 5. However, it is apparent that de-activation in light, while exposed to low pressure, is much faster than de-activation in air with no light. The data of Figure 6(a) also exhibits an envelope to the activation/de-activation

cycles. The maxima of Figure 6(a) appear to define a curve similar to the activation curve of Figure 2(b). The minima trace out a curve that appears to rise exponentially and reach a quasi-asymptotic value after 10 cycles. Both of these observations imply that the activation is not completely reversible. This is not surprising since we observe a blue-shift of the exciton luminescence spectrum (Figure 3), which implies an irreversible photooxidation of the quantum dot. The fact that the luminescence does not recover to the same value in a vacuum (i.e. the minimum points) suggests that some of the adsorbates remain on the quantum dot and are not removed by the vacuum in the time scale of the experiment. This could be an indication of photodissociative adsorption. Dissociative adsorption has been recently suggested by NMR for H₂O adsorbed on un-passivated CdS quantum dots.²⁵ In these experiments, we conclude that both physisorbed H₂O molecules as well as chemisorbed OH groups and H atoms exist on the quantum dot surface, and that evacuation does not remove all of the adsorbed species.

Figure 6(b) shows the evolution of the deep trap emission during our pressure cycling experiment. The data of Figure 6(b) show that when the exciton emission rises with simultaneous exposure to air and light, the deep trap emission falls. When the sample chamber is evacuated and the surface adsorbates are removed, the exciton luminescence falls and the deep trap emission rises. This implies that the adsorbed water molecules responsible for increasing the exciton emission are also responsible for decreasing the defect emission. In addition, the envelope of the data of Figure 6(b) shows a steady, nearly linear increase in the deep trap emission (both for the minima and maxima) as the number of cycles are increased. This indicates that the decrease of the deep trap emission also has an element of irreversibility, and suggests that the density of defects increases with accumulated exposure time in air.

IV. Discussion and Conclusions

We have shown that the large decrease in QY upon the formation of a 2-D close-packed solid is recovered upon exposure to above band edge illumination. Our data strongly suggests that surface adsorbates, specifically water molecules, are responsible for the luminescence activation. A model suggested by these data (see Figure 7) is that the water molecules adsorb to the surface of the quantum dots during illumination, and passivate surface traps. The surface traps that are passivated are responsible for quenching the exciton emission of the monolayer in a vacuum as well as for the weak defect emission in the red region of the luminescence spectrum (see Figure 2(b)). During the early illumination times (within 10 s), the exciton emission increases and the defect emission decreases (see Figure 6) consistent with the density of defects decreasing as the concentration of surface adsorbates increases. The decrease in the rms width of the spectrum can also be explained in the context of a change in the size distribution of the quantum dots. We know from the data of Figure 4a that smaller diameter quantum dots (<3 nm) photooxidize much more rapidly than the larger diameter quantum dots. It is possible that the initial decrease in the rms width is due to the removal of the smaller-size quantum dots via rapid photooxidation, which narrows the size distribution. The subsequent increase in the rms width is then due to the partial recovery of the initial distribution as the larger quantum dots are oxidized.

The increase in luminescence QY due to adsorbed molecules on the quantum dot surface is similar to the widely studied enhancement of the luminescence QY observed upon adsorption of electron-donating molecules (Lewis bases) to bulk CdSe

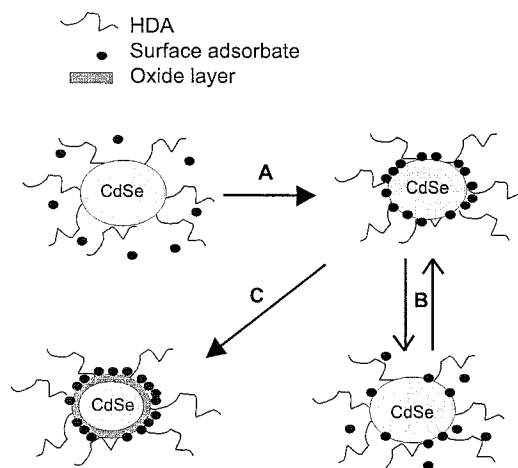


Figure 7. Simple illustration of the proposed adsorption model for the luminescence activation. Nearby water molecules adsorb to the surface of the quantum dot upon illumination with above band edge light (path A). The adsorption is pseudo-reversible shown by path B. Here, the adsorbates are removed during illumination by opening the sample to vacuum, or likewise by shuttering the illumination source off in room air. Path C shows the eventual outcome of extended excitation in air. Consequently, the formation of an oxide layer leads to a decrease in the luminescence, and a smaller dot (blue shift in the exciton spectrum). The product of path C can continue to undergo path B as evident in Figure 5, but is not illustrated here.

surfaces.²² There are, however, significant differences between the luminescence activation observed for quantum dot and bulk CdSe surfaces. First, the luminescence increase for bulk surfaces is generally attributed to a decrease in the thickness of the “dead layer” of the CdSe surface.²² This dead layer results from the high density of mid-gap states at the surface, which arise from surface defects. For bulk CdSe, this dead layer is on the order of 100 nm thick, more than an order-of-magnitude larger than the diameter of a CdSe quantum dot. Our data suggest that the surface states passivated by the water molecules most likely come from the first layer of atoms. Second, the kinetics of the luminescence activation is more complicated than the first-order (single exponential) kinetics observed for bulk CdSe surfaces, since the luminescence QY eventually decreases instead of reaching an asymptotic level. Our data suggest that the adsorbed molecules react with the CdSe quantum dot surface, create an oxide layer, and result in a smaller diameter quantum dot. This reduction in diameter is manifested in our data as a blue shift in the exciton emission spectrum.

In addition, we attribute the eventual decrease of luminescence QY at long illumination times to the formation of the surface oxide. Oxidation of bulk CdSe surface is known to be unstable and to create surface defects. Photooxidation of the quantum dots will therefore create new defects which both quench the exciton emission resulting in a lower luminescence QY.

In summary, we attribute the complex kinetics of both the luminescence QY and the rms width of the exciton emission to a competition between the passivation of surface defects by adsorbed water molecules which increases the luminescence efficiency and photooxidation of the quantum dot which decreases the luminescence efficiency. We also note that our model is not limited to quantum dot monolayers. We have observed the activation phenomenon in colloids exposed to air, three-dimensional quantum dot solids, quantum dots embedded in polymers and sol-gel glasses, and even for a single isolated quantum dot on a glass surface. We are continuing to investigate

this phenomenon on different structures, as a function of quantum dot size and as a function of the capping ligand.

Acknowledgment. The authors thank Stephanie Chaney for colloid QY data, Dr. Gernot Wirsberger for use of the integrating sphere, and Dr. Chang Ryu for help acquiring the TEM images. S.K.B. acknowledges support from the Lucile and David Packard Foundation. This work was also supported by an NSF Nanotechnology grant.

References and Notes

- (1) Bawendi, M. G.; Steigerwald, M. L.; Brus, L. E. *Annu. Rev. Phys. Chem.* **1990**, *41*, 477–496.
- (2) Bawendi, M. G.; Carroll, P. J.; Wilson, W. L.; Brus, L. E. *J. Chem. Phys.* **1992**, *96*, 946–954.
- (3) Empedocles, S.; Bawendi, M. *Acc. Chem. Res.* **1999**, *32*, 389–396.
- (4) Heath, J. R. *Science* **1995**, *270*, 1315–1316.
- (5) Tittel, J.; Gohde, W.; Koberling, F.; Basche, T.; Kornowski, A.; Weller, H.; Eychmuller, A. *J. Phys. Chem. B* **1997**, *101*, 3013–3016.
- (6) Katari, J. E. B.; Colvin, V. L.; Alivisatos, A. P. *J. Phys. Chem.* **1994**, *98*, 8, 4109–4117.
- (7) Nirmal, M.; Dabbousi, B. O.; Bawendi, M. G.; Macklin, J. J.; Trautman, J. K.; Harris, T. D.; Brus, L. E. *Nature* **1996**, *383*, 802–804.
- (8) Nirmal, M.; Brus, L. *Acc. Chem. Res.* **1999**, *32*, 407–414.
- (9) Brus, L. *Appl. Phys.* **1991**, *53*, 465–474.
- (10) Collier, C. P.; Vossmeier, T.; Heath, J. R. *Annu. Rev. Phys. Chem.* **1998**, *49*, 371–404.
- (11) Mikulec, F. V.; Kuno, M.; Bennati, M.; Hall, D. A.; Griffin, R. G.; Bawendi, M. G. *J. Am. Chem. Soc.* **2000**, *122*, 2532–2540.
- (12) Murray, C. B.; Norris, D. J.; Bawendi, M. G. *J. Am. Chem. Soc.* **1993**, *115*, 8706–8715.
- (13) Murray, C. B.; Kagan, C. R.; Bawendi, M. G. *Science* **1995**, *270*, 1335–1338.
- (14) Micic, O. I.; Jones, K. M.; Cahill, A.; Nozik, A. J. *J. Phys. Chem. B* **1998**, *102*, 9791–9796.
- (15) Dabbousi, B. O.; Murray, C. B.; Rubner, M. F.; Bawendi, M. G. *Chem. Mater.* **1994**, *6*, 216–219.
- (16) Kagan, C. R.; Murray, C. B.; Nirmal, M.; Bawendi, M. G. *Phys. Rev. Lett.* **1996**, *76*, 1517–1520.
- (17) Kagan, C. R.; Murray, C. B.; Bawendi, M. G. *Phys. Rev. B* **1996**, *54*, 8633–8643.
- (18) Peng, X. G.; Schlamp, M. C.; Kadavanich, A. V.; Alivisatos, A. P. *J. Am. Chem. Soc.* **1997**, *119*, 7019–7029.
- (19) Kuno, M.; Lee, J. K.; Dabbousi, B. O.; Mikulec, F. V.; Bawendi, M. G. *J. Chem. Phys.* **1997**, *106*, 9869–9882.
- (20) Tian, Y. C.; Wu, C. J.; Fendler, J. H. *J. Phys. Chem.* **1994**, *98*, 4913–4918.
- (21) Brainard, R. J.; Ellis, A. B. *J. Phys. Chem. B* **1997**, *101*, 2533–2539.
- (22) Kepler, K. D.; Lisensky, G. C.; Patel, M.; Sigworth, L. A.; Ellis, A. B. *J. Phys. Chem.* **1995**, *99*, 16 011–16 017.
- (23) Khitrov, G. A.; Simburger, J. T.; Raola, O.; Strouse, G. F. Submitted for publication, 3/2000.
- (24) Greenham, N. C.; Samuel, I. D. W.; Hayes, G. R.; Phillips, R. T.; Kessener, Y. A. R. R.; Moratti, S. C.; Holmes, A. B.; Friend, R. H. *Chem. Phys. Lett.* **1995**, *241*, 89.
- (25) Ladizhansky, V.; Hodes, G.; Vega, S. *J. Phys. Chem. B* **2000**, *104*, 1939–1943.